STRESS CORROSION CRACKING MECHANISMS OF FE-BASED ALLOYS IN HYDROGENATED HOT WATER

Z. COULL

Dept. of Chemical Engineering & Applied Chemistry, University of Toronto, 200 College St, Toronto, M5S 3E5
Tel: 416-946-0637. Email: zcoull@chem-eng.utoronto.ca

It is generally accepted that carbon steel resists Stress Corrosion Cracking (SCC) in hot water provided the oxygen content is low enough[1]; however, isolated cracking events have occurred[2], apparently in fully reducing conditions, and these may or may not be true SCC. There are also occasional reports of SCC of austenitic stainless steel in reducing conditions[3] where cold work may play a critical role. SCC though originally seen in sensitized material at oxidizing potentials persists to low potentials and in cold-worked but unsensitized material.

We suspect from the literature that alloying with Ni introduces a susceptibility to SCC in reducing hot water as well as in caustic solution[4]. Our hypothesis is that Ni causes SCC, and Cr retards it; so stainless steel has just enough Cr to protect against SCC under most conditions. We are examining this using model Fe-based materials and environments designed to separate the effects of different parameters.

Early results suggest that Fe-Ni alloys and austenitic SS both undergo de-alloying and SCC in reducing caustic solutions. It is hypothesised that if these alloys are indeed susceptible to dealloying (and hence to SCC) in this environment then we can reasonably project that their behaviour in reducing, hot pure water may be similar. This is pertinent to understanding recent failures in high temperature, high pressure aqueous systems. As a first step we have investigated the surface reactions that occur in caustic solutions and in hot water.

Key Words: stress corrosion cracking, dealloying, high temperature water

Mechanistic Background

One mechanism of Stress Corrosion Cracking (SCC) involves film induced cracking where a nanoporous or otherwise brittle surface film on a material triggers a brittle substrate microcrack under a stress[5,6]. Dealloying (selective dissolution) can provide such a layer on the surface. The resulting dealloyed layer is not only brittle but is coherent with the metal lattice and, as such, a crack can more easily propagate into the metal.

Dealloying requires that a number of threshold barriers are overcome and these are a function of the alloy composition and the electrochemical potential:

- The components in an alloy must display significantly different metal/metal-ion equilibrium potentials and thus dissolution rates in the medium in question[7] e.g. silver-gold alloys, brasses etc. In addition, a critical electrochemical potential must be reached where sufficient active material can be dissolved; below this potential the surface ‘passivates’ with a continuous layer of the more noble component.

- In order to initiate a crack the dealloyed layer must be of sufficient thickness[5] ; however it is suggested by Friedersdorf and Sieradzki[6] that there is an upper limit to the thickness too. Presumably there is an optimal thickness range where the dealloyed layer maintains enough lattice coherency to induce propagation.

In order to better understand the boundaries of the Fe-Ni-Cr SCC map, shown in Figure 1, this work will start by examining dealloying type behaviour of a variety of Fe-Ni alloys in reducing, hot caustic solutions. Echoes of this behaviour will be sought in reducing, high temperature water environments.

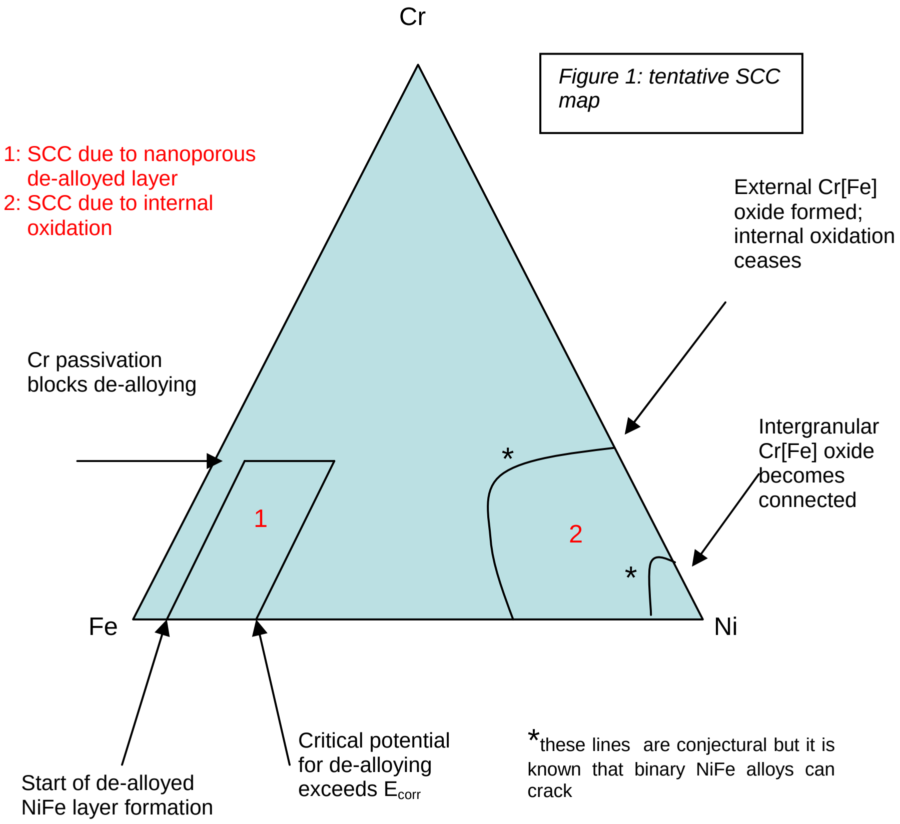

Figure 1: tentative SCC map

1: SCC due to nanoporous de-alloyed layer
2: SCC due to internal oxidation

External Cr[Fe] oxide formed; internal oxidation ceases

Cr passivation blocks de-alloying

Intergranular Cr[Fe] oxide becomes connected

Start of de-alloyed NiFe layer formation

Critical potential for de-alloying exceeds E_{corr}

*these lines are conjectural but it is known that binary NiFe alloys can crack

Materials and Experimental Procedures

Materials

A variety of materials were used for this investigation: Fe, Ni, Fe10%Ni and Fe50% Ni. These materials were prepared by mechanical polishing to at least 1200 grit.

Low Temperature Corrosion Studies

Corrosion studies were carried out in 100ml of 20% and 30% sodium hydroxide (NaOH) solution. Deaeration was achieved by purging the solution with nitrogen for 20 minutes prior to each test. The solution in the beaker was heated via a double walled cell containing 80% glycol. Heating was achieved by heating the solution on a hot plate and temperature allowed to stabilise for 2 hours prior to testing.

An all-PTFE mercury / mercurous oxide (Hg/HgO) reference electrode was connected to the cell via an all-PTFE salt bridge and was used to measure potential and control the electrochemistry.

The counter electrode consisted of platinum wire which wound around a PTFE holder and placed in the cell close to the sample.

Electrochemical Techniques

All electrochemistry was done using the capabilities of the PARSTAT 2263 Advanced Electrochemical System:

- Cyclic polarization (CP) curves were measured at a scan rate of 3 mV/s. This gave general information about the corrosion behaviour of each material.

- Electrochemical Impedance Spectroscopy (EIS) scans measure electrochemical impedance over a range of AC frequencies and can allow the determination of double layer capacitance (C_{dl}). C_{dl} is proportional to the real surface area of a material and, if measured over time, can indicate the presence of a porous dealloyed layer[4]. The ac voltage amplitude was 10 mV_{rms} and the frequency range was 4 kHz to 100 mHz. Electrochemical capacitances are not pure, can be masked by diffusional effects, and generally show some frequency dispersion (e.g. phase angle of -80 instead of -90 degrees), thus we quote the capacitance at a particular frequency where reasonable capacitive behaviour was observed; this was not always the same range.

High Temperature Corrosion Studies

Exposure studies and electrochemistry were also carried out on Fe10Ni in hydrogenated, solutions at 250°C within an autoclave using a Platinized Niobium reference electrode. Samples were electrochemically examined using CP and EIS (as at low temperature) to determine any changes in behaviour. In hot water environments with hydrogen, it is likely that any Ni enrichment (dealloying) process will require much longer exposure times. In order to accelerate the behaviour, solutions containing small concentrations of ions have been used to increase conductivity and decrease pH. Exposure times have also been extended and the material has been held at anodic potentials, such as +80mV vs. initial OCP, to promote active dissolution of Fe, simulating a low-oxygen or not-quite reducing, contaminated hot-water environment.

Results and Discussion

Figures 2 and 3 show the cyclic polarisation behaviour of Fe10Ni and Fe50Ni respectively in 30% NaOH at 110°C. The curve for Fe10Ni shows two distinct current peaks which correlate to the active–passive transitions for Fe and Ni. The potential region between -850 and -920 mV corresponds to an active dissolution or dealloying region. This feature is not seen in the Fe50Ni material. In this case the material appears to behave more like pure Ni (not shown) although there is some evidence of a depressed Fe active peak. For Fe-50Ni, the critical potential for de-alloying is higher than the potential where Ni starts to oxidize.

Figure 2: CP of Fe10Ni in deaerated 30%NaOH at 110°C

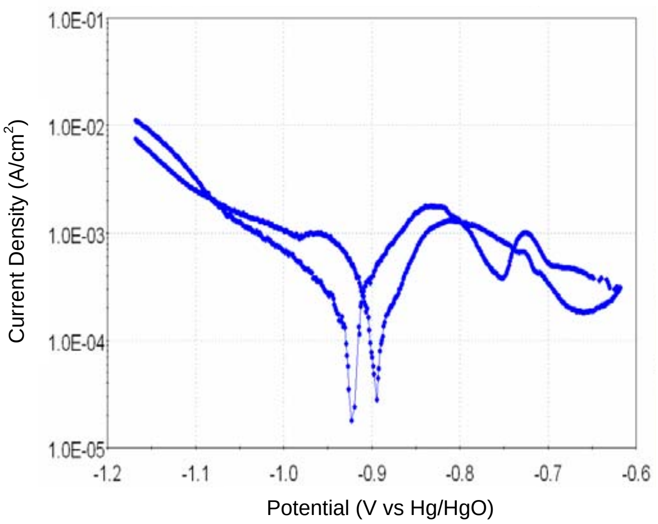

Figure 3: CP of Fe50Ni in deaerated 30%NaOH at 110°C

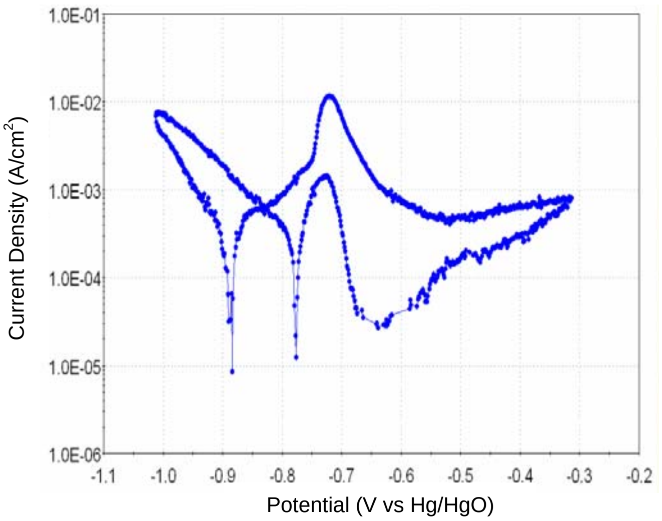

Figure 4: CP of Fe10Ni in hydrogenated (10^{-3}M Na_2SO_4 + 10^{-2}M H_3BO_3) at 250°C (held at +80mV vs. initial OCP for immersion duration)

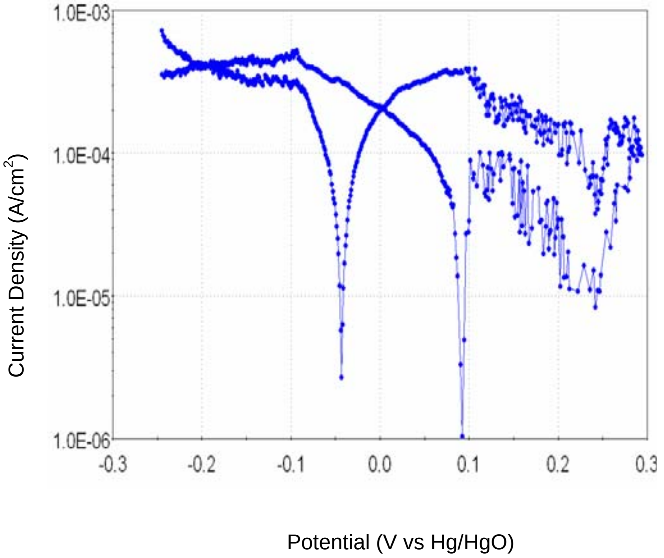

Figure 4 shows the cyclic polarisation behaviour of Fe10Ni in 10^{-3}M Na_2SO_4 + 10^{-2}M H_3BO_3 solution at 250 °C after an immersion time of 16 hours. It can be seen that there are no longer two distinct active peaks for Fe and Ni. It is likely that in this environment any dealloying potential range will be very narrow due to the similar electrochemical behaviour of these elements and may in fact be quite difficult to isolate. Further work will require the use of longer times and different potentials.

Figure 5 shows capacitance versus time (at OCP) for Fe10Ni in 30%NaOH at 110°C. The capacitances were calculated manually from log Z_{im} vs. log (omega) plots. It can be seen from these data that there is a marked increase in capacitance for the Fe10Ni material. This is consistent with the dc electrochemistry indicating that Fe10Ni is dealloying. This was not seen for Fe50Ni (not shown) which again mimics the behaviour of Ni (not shown).

Figure 5: Capacitance vs time (Fe10Ni in 30% NaOH at 110°C)

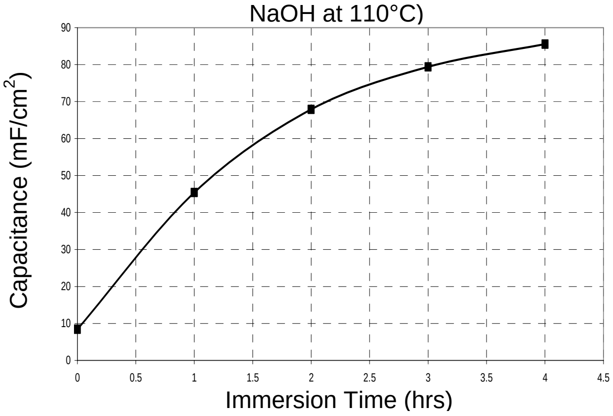

Figure 6: Capacitance vs time (Fe10Ni in hydrogenated 10^{-3}M Na_2SO_4 + 10^{-2}M H_3BO_3 at 250°C)

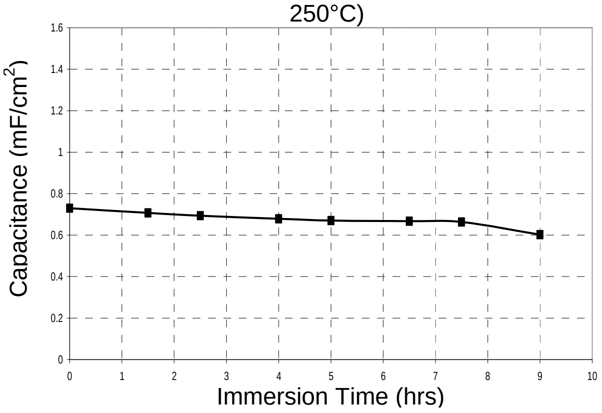

Figure 6 shows capacitance versus time (held at an anodic potential of +80mV for the experiment duration) for Fe10Ni in 10^{-3}M Na_2SO_4 + 10^{-2}M H_3BO_3 at 250°C. It can be seen from these data that there is no significant change in capacitance over time.

Conclusions

From these comparisons it is unclear at this stage if the behaviour of Fe-Ni alloys in high temperature, reducing water environments can be treated as the dilute limit of the dealloying behaviour seen in caustic solutions. It is likely that any Ni enrichment is more subtle and 'solid-state', and may take longer immersion times to appear. Consequently future experimentation will continue to systematically increase the severity of the experimental conditions, with respect to temperature and pH in order to attempt to accelerate possible processes. Dealloying may also appear either at higher potentials or with static or perhaps dynamic plastic deformation. Cross-sectional microscopy and surface analysis may also help to identify the location and role of Ni in these surfaces.

Acknowledgements

This research was supported by NSERC (Canada) and by UNENE, the University Network of Excellence in Nuclear Engineering. The author would like to thank Prof. R. C. Newman for his guidance and supervision and Dr. Anatolie Carcea for his assistance with EIS analysis.

References

1. M.O. Speidel and R.M. Magdowski, ‘Stress Corrosion Cracking of Nuclear Reactor Pressure Vessel and Piping Steel’, *Int. J. Press. Vess. & Piping,* **Vol. 34**, pp 119-142 (1988).

2. J. Slade and T. Gendron, ‘Flow Accelerated Corrosion and Cracking of Carbon Steel Piping in Primary Water – Operating Experience at the Point Lepreau Generating Station’ in *Conf. Proc.* 12th International Conference on Environmental Degradation in Nuclear Power Systems – Water Reactors, Salt Lake City, (August 2005).

3. F. P. Ford and P. L. Andresen, 'Corrosion in Nuclear Systems: Environmentally Assisted Cracking in Light Water Reactors', in *Corrosion Mechanisms in Theory & Practice,* ed. P Marcus, Marcel Dekker Inc, New York, 2nd Ed, pp 605-642 (2002).

4. J. Deakin, Z. Dong, B. Lynch and R.C. Newman, 'Dealloying of Type 316 Stainless Steel in Hot, Concentrated Sodium Hydroxide Solution', *Corrosion Science*, **Vol. 46,** pp 2117-2133 (2004).

5. K. Sieradzki and R.C. Newman, ‘Stress corrosion cracking’, *J. Phys. Chem. Solids*, **Vol. 48**, pp 1101-1113 (1987).

6. F. Friedersdorf and K. Sieradzki, ‘Film-Induced Brittle Intergranular Cracking of Silver-Gold Alloys’, *Corrosion*, **Vol. 52,** pp 331-336 (1996).

7. J. Erlebacher and K. Sieradzki, ‘Pattern formation during dealloying’, *Scripta Materialia,* **Vol. 49,** pp 991–996 (2003).